Revisiting the relationship between solar X-ray irradiance and magnetic flux using Hinode/XRT, SDO/HMI, and SOHO/MDI

Keiji Yoshimura, Aki Takeda, Dana W. Longcope (Montana State Univ.)

Abstract

The relationship between total unsigned magnetic flux and X-ray spectral luminosity was notably studied by Pevtsov et al. (2003). Their analysis used over 12 orders of magnitude in flux, ranging from quiet region of the Sun through T Tauri stars. From this data they concluded that a single power-law (index = 1.15) could well express the relationship for the whole range (Fig.1). They also reported that the power-law index for the full, disk-integrated flux changes from the low magnetic flux end (index ~2) to high end (index ~1), which forms a "knee" in the plot of X-ray luminosity vs magnetic flux. The solar full disk portion of their study was based on the X-ray data from Yohkoh/SXT (Al.1 and AlMg filters) and magnetic flux data from NSO/Kitt Peak.

We utilized more recent datasets, Hinode/XRT and SDO/HMI magnetograms, to confirm whether there is the same change of the power-law index for the full Sun data and to evaluate the stability of the relationship through various parameters.

The parameters we checked are:
(1) selection of XRT filter pairs,
(2) area of integration,
(3) energy band of irradiance calculation,
(4) different version of CHIANTI,
(5) coronal abundance model, and
(6) cutoff magnetic field strength.

All the results show single or broken power law distribution. We found the cutoff magnetic field strength was the key parameter of the "knee" structure. The "knee" can be seen with the low cutoff values, but not with the higher values. The critical value appears to be higher than the noise level of the HMI magnetograph. This may suggest there are weak magnetic field which do not contribute to the X-ray luminosity.

Data/Method

[X-ray Luminosity *Lx*]

- XRT data in the Synoptic Composite Image Archive (Takeda et al. 2016)
- Mainly use "Alpoly" and "ThinBe" filter pairs

(1) X-ray fluxes are calculated by summing up all the counts of the pixels within a specific distance (***Rx***) from the disc center
(2) Derive temperature(*Te*) and emission measure(*EM*) from the X-ray fluxes by filter ratio method (Vaiana et al. 1973)
(3) Calculate isothermal coronal spectrum from the *Te* and *EM*
(4) Integrate the spectrum over the wavelength range (2.8-36.6A) to get X-ray luminosity
(5) Averaged taken over one day

[Unsigned Total Magnetic Flux *Mx*]

- 720 sec cadence HMI magnetogram

(1) Correct projection effect, assuming all the magnetic field are radial
(2) Sum up unsigned magnetic fluxes of all the pixels showing stronger magnetic field than ***Bc*** within a specific distance ***Rm*** from the disc center
(3) Averaged taken over one day

[1] Rx, Rm *(Bc=60G, Al_poly – Thin_Be)*

We obtain single power law distributions with these parameters. Correlation coefficient of Lx and Mx were calculated for various Rx and Rm pairs (Fig.3). The pair Rx=0.83Rsun, Rm=0.79Rsun maximize the coefficient. We use the values close to the pair for the calculation below.

[2] CHIANTI, abundance model *(Bc=60G, Al_poly – Thin_Be)*

The results using different CHIANTI versions (9.0.1 or 10.0.0) and different abundance mode (corona or hybrid) are in Fig.4. There are no major change. We use CHIANTI ver. 10.0.0 with "corona" abundance for the calculation below.

[3] XRT filter pairs *(Bc=60G)*

Some different choices of filter pairs result in small difference of power law indices (Fig.5), though there are no major change in the distribution.

In Fig.5x (Ti_poly and Be_thin pairs) data points of lower end are missing due to the lack of useful observation during the solar minimum phase.

[4] Energy Bin *(Bc=60G, Al_poly - Thin_Be)*

While the sensitivity range of the SXT is 2.8-36.6A, that of the XRT (Al_poly filter) extends to longer wavelengths (Fig.6). We integrated over the range 5-50A and made the same plot. We get a slightly smaller power law index (Fig.7).

Note that Toriumi and Airapetian (2022) reported the power law indices are lower for the longer wavelength radiation.

[5] Bc *(Al_poly - Thin_Be)*

The results from different Bc are in Fig.8. The transition from "broken power law" to "single", and back to "broken", can be seen by an increase of Bc. We obtain the single power law distribution when Bc falls in the range of 50-75G. The power law index in the range are ~1 (1.03 - 1.16).

The value 50-75G is higher than the noise level of the HMI magnetograph (sigma=5-6G). If we assume "single power law" is the "right" one, this may suggest there are weak magnetic field which do not contribute to the X-ray luminosity.

[6] Kitt Peak v.s. SXT

We applied the same method to the data set in Pevtsov et al. (2003) to confirm if we can obtain the same transition (single to broken to single). Fig.9 shows that the transition occurs in lower Bc (< 20G).

Note that the spatial resolution of Kitt Peak data is lower than that of HMI (Fig.10). If the HMI data are blurred (5x5 smoothing) to resemble Kitt Peak data, we obtain lower Bc value for the transition (Fig.11). So the results are all consistent.

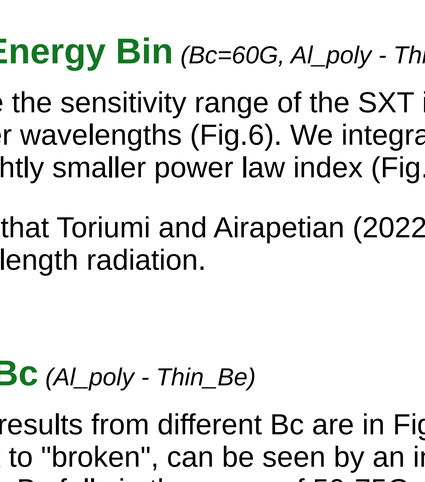

Fig.10

Magnetogram os Quiet Sun region from Kitt Peak (upper left) and HMI (upper right). The lower panel shows the same HMI data with smoothing 5x5 pixels.

References
Narukage et al. 2011, Sol.Phys., 269, 169
Pevtsov et al. 2013, ApJ, 598, 1387
Takeda et al. 2016, Sol.Phys., 291, 317
Toriumi and Airapetian 2022, ApJ, 927, 179
Vaiana et al. 1973, Sol.Phys., 1, 81

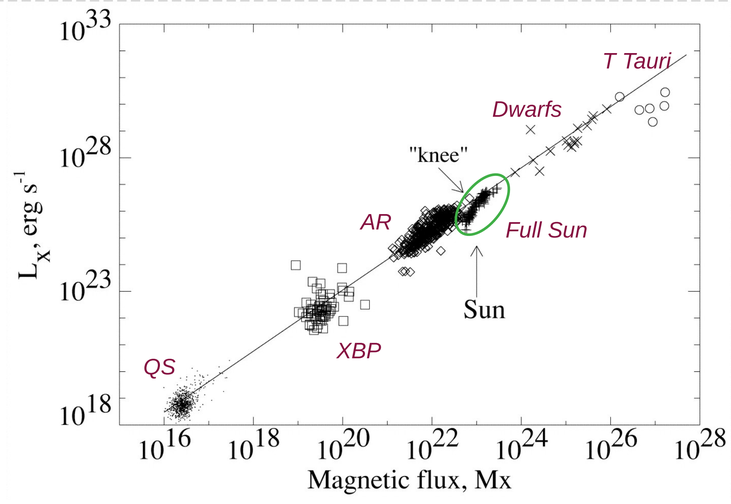

Fig.1
From Pevtsov et al (2003)

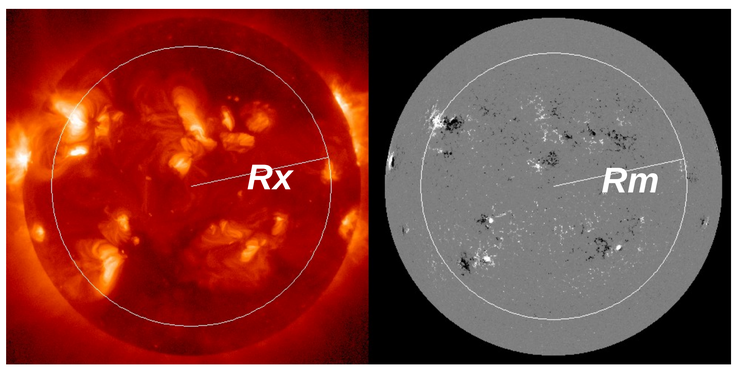

Fig.2
Samples of XRT Al_poly and HMI magnetogram taken on 2013/01/08.

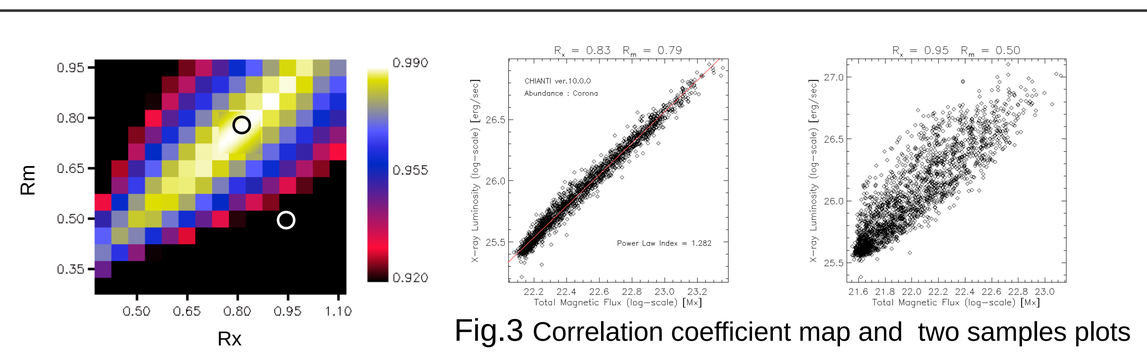

Fig.3 Correlation coefficient map and two samples plots

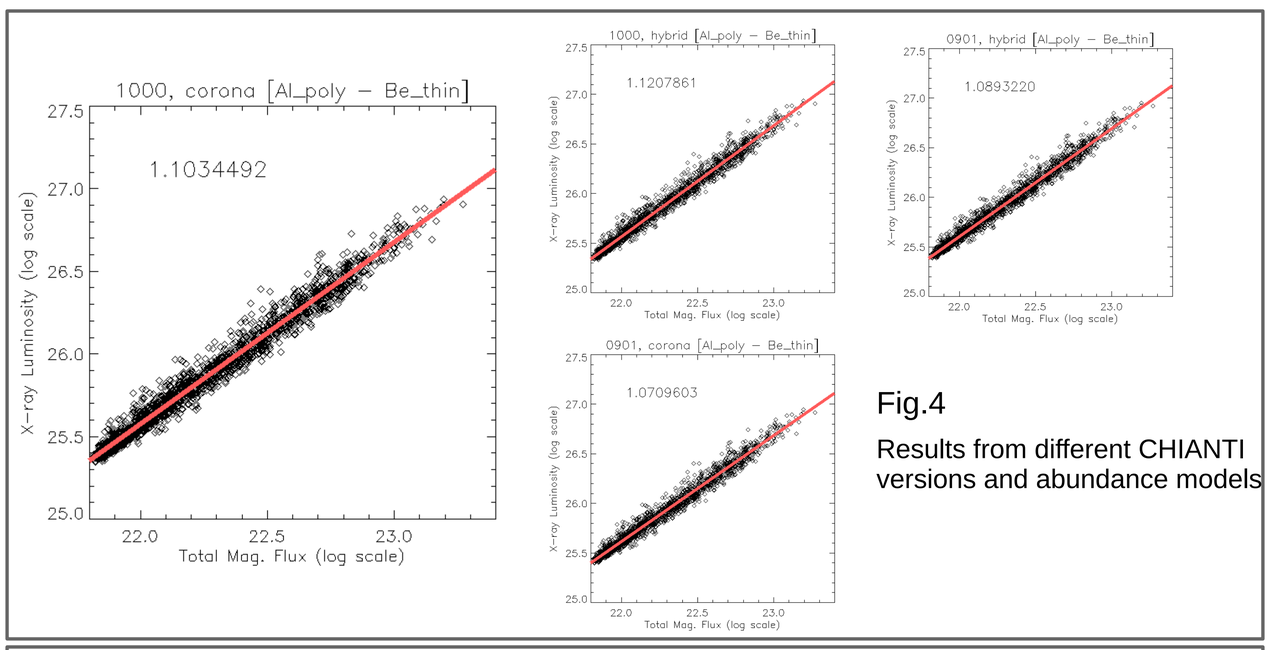

Fig.4
Results from different CHIANTI versions and abundance models

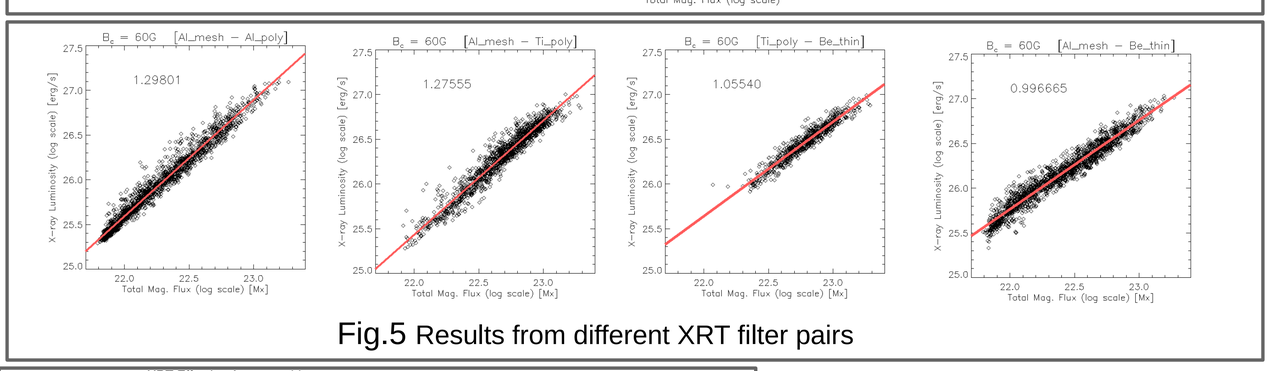

Fig.5 Results from different XRT filter pairs

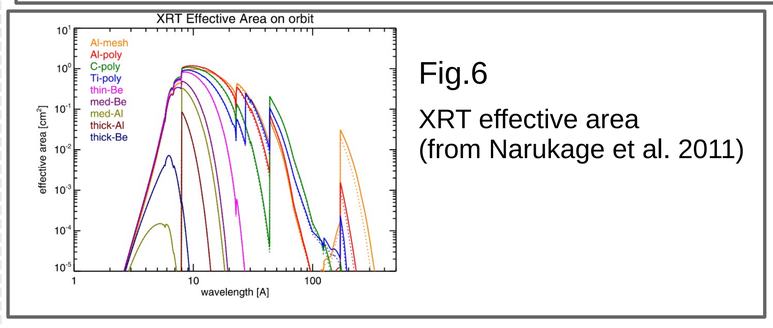

Fig.6
XRT effective area
(from Narukage et al. 2011)

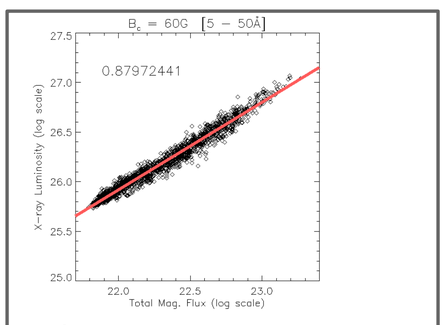

Fig.7
Results from different X-ray wavelength range (5-50A)

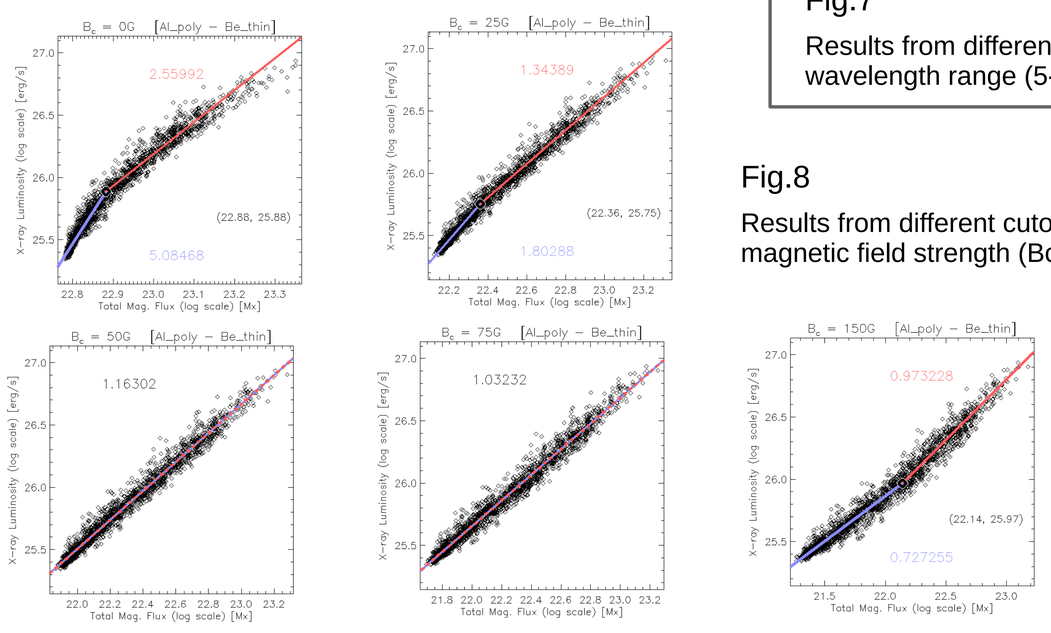

Fig.8
Results from different cutoff magnetic field strength (Bc)

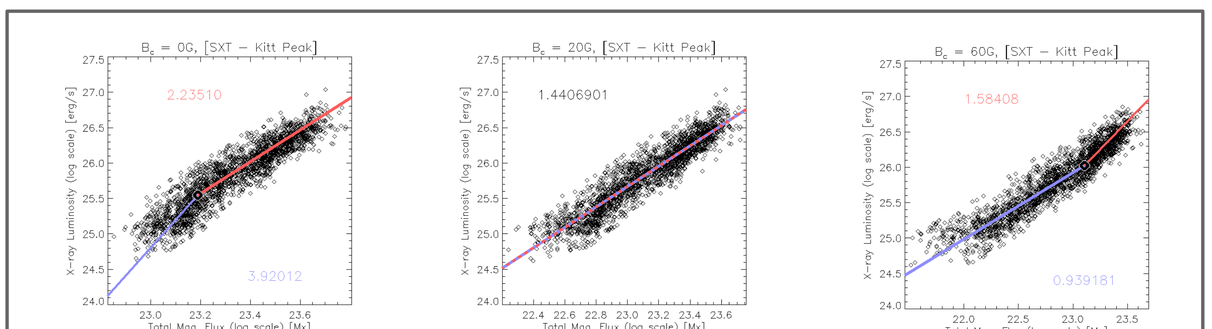

Fig.9 Results from different cutoff magnetic field strength (Bc) using SXT data and Kitt Peak magnetograms

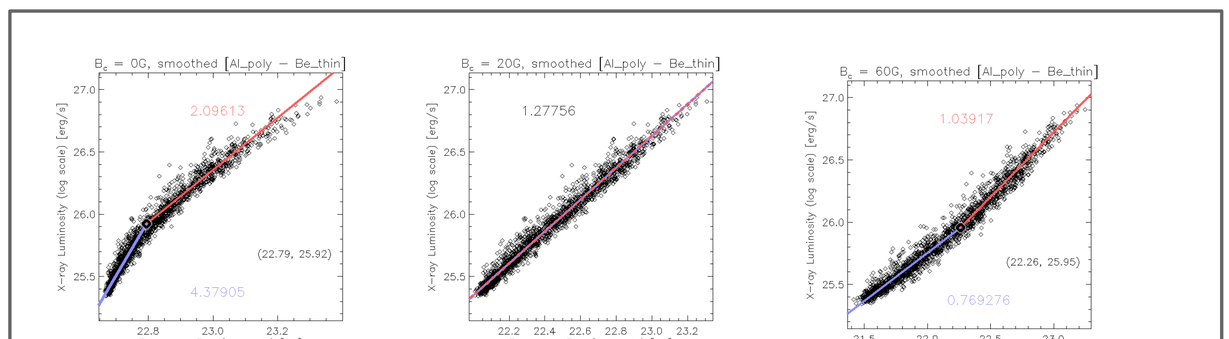

Fig.11 Results from different cutoff magnetic field strength (Bc) using XRT data and smoothed HMI magnetograms